HHS Public Access

Author manuscript

Sci Signal. Author manuscript; available in PMC 2017 January 12.

Published in final edited form as:

Sci Signal. ; 9(456): ra117. doi:10.1126/scisignal.aai8441.

Biased agonists of the kappa opioid receptor suppress pain and itch without causing sedation or dysphoria

Tarsis F. Brust[1], **Jenny Morgenweck**[1], **Susy A. Kim**[2], **Jamie H. Rose**[3], **Jason L. Locke**[3], **Cullen L. Schmid**[1], **Lei Zhou**[1], **Edward L. Stahl**[1], **Michael D. Cameron**[1], **Sarah M. Scarry**[4], **Jeffrey Aubé**[4], **Sara R. Jones**[3], **Thomas J. Martin**[2], and **Laura M. Bohn**[1,*]

[1]Departments of Molecular Therapeutics and Neuroscience, The Scripps Research Institute, Jupiter, FL 33458, USA

[2]Department of Anesthesiology, Wake Forest School of Medicine, Winston-Salem, NC 27157, USA

[3]Department of Physiology and Pharmacology, Wake Forest School of Medicine, Winston-Salem, NC 27157, USA

[4]Division of Chemical Biology and Medicinal Chemistry, UNC Eshelman School of Pharmacy, University of North Carolina at Chapel Hill, Chapel Hill, NC 27599, USA

Abstract

Agonists targeting the kappa opioid receptor (KOR) have been promising therapeutic candidates because of their efficacy for treating intractable itch and relieving pain. Unlike typical opioid narcotics, KOR agonists do not produce euphoria or lead to respiratory suppression or overdose. However, they do produce dysphoria and sedation, side effects that have precluded their clinical development as therapeutics. KOR signaling can be fine-tuned to preferentially activate certain pathways over others, such that agonists can bias signaling so that the receptor signals through G proteins rather than other effectors such as βarrestin2. We evaluated a newly developed G protein signaling–biased KOR agonist in preclinical models of pain, pruritis, sedation, dopamine regulation, and dysphoria. We found that triazole 1.1 retained the antinociceptive and antipruritic efficacies of a conventional KOR agonist, yet it did not induce sedation or reductions in dopamine release in mice, nor did it produce dysphoria as determined by intracranial self-stimulation in rats. These data demonstrated that biased agonists may be used to segregate physiological responses downstream of the receptor. Moreover, the findings suggest that biased KOR agonists may present a means to treat pain and intractable itch without the side effects of dysphoria and sedation and with reduced abuse potential.

*Corresponding author. lbohn@scripps.edu.

Author contributions: T.F.B. conducted the cell-based assays. T.F.B. and E.L.S. performed the bias analysis. T.F.B., J.M., and C.L.S. performed the behavioral experiments for antinociception, pruritis, and locomotor activity. L.Z. and E.L.S. performed radioligand occupancy studies. J.A. provided medicinal chemistry expertise. S.M.S. developed large-scale synthesis and synthesized triazole 1.1. M.D.C. measured brain levels of compounds. S.R.J. designed and J.H.R. and J.L.L. performed the dopamine neurochemistry studies in mouse. T.J.M. designed and S.A.K. performed the ICSS studies in rat. L.M.B., J.A., S.R.J., and T.J.M. conceived the study and analyzed their respective contributions. L.M.B. wrote the manuscript with contributions from the rest of the authors.

Competing interests: The other authors declared that they have no competing interests.

INTRODUCTION

The kappa opioid receptor (KOR) is a G protein–coupled receptor (GPCR) that is distributed throughout the nervous system and is activated by opioid peptides, such as dynorphins (1–3). Like other opioid receptors, its activation promotes antinociception, and therefore, it has been a target for development of pain therapeutics (4). KOR agonists have also been proven to be efficacious in the treatment of intractable, non–histamine-related itch, or pruritis (5–8). Currently, nalfurafine is the only clinically available KOR agonist, and it is used in the treatment of pruritis (9). In addition to providing pain relief without the threat of overdose, KOR agonists are unlikely to be addictive because they do not induce euphoria, nor do they promote increases in dopamine release, as abused drugs do (10–12).

However, activation of KOR on dopaminergic nerve terminals leads to decreases in extracellular dopamine concentrations in mice and rats (13, 14). It is believed that this drop in dopamine is responsible for the dysphoric effects produced by KOR agonists (12, 15–19). To bypass such adverse side effects, one approach has been to develop KOR agonists that do not penetrate the blood-brain barrier in an attempt to isolate their actions to peripheral sites for the treatment of pain (5). However, KOR modulation of central limbic circuits may play a substantial role in pain processing, particularly regarding the affective component of pain and the comorbidity of chronic pain and depression (20). Therefore, restricting KOR to peripheral pain regulation may limit efficacy and limit the types and severity of pain that could be treated by targeting this receptor system.

Another approach would be to selectively activate KOR such that it suppresses pain perception yet does not produce dysphoria or decrease dopamine concentrations. It has become increasingly evident that GPCRs signal differently in different contexts and that these properties, if understood, could be used to refine therapeutics (21). For example, a receptor in a GABAergic neuron may signal through a $G\alpha_{i/o}$ signaling pathway to disinhibit transmission, whereas a receptor in a dopaminergic neuron may use another signaling pathway to promote dopamine release. This sort of receptor signaling, which has been termed biased agonism or functional selectivity, can be harnessed by developing ligands that promote one favorable signaling interaction over another (22).

For the KOR, there is genetic and pharmacological evidence to support that functional selectivity is possible (8, 19, 23–26). GPCR signaling diverges at key proximal signaling points, occurring at the level of multiple heterotrimeric G protein coupling options as well as a second major avenue, having a direct interaction with βarrestins (22, 27, 28). As scaffolding proteins, βarrestins promote interactions with kinases independent of GPCR–G protein interactions to induce downstream signaling (28, 29). Studies in mice that lack G protein–coupled receptor kinase 3 (GRK3), a kinase that phosphorylates GPCRs and promotes βarrestin interactions, provide evidence that a GRK3/βarrestin–facilitated pathway underlies the inhibitory dopaminergic responses to KOR agonists because these mice do not display aversion-related behaviors in response to conventional KOR agonists (19, 23).

Here, we use a KOR-selective agonist that preferentially activates KOR-mediated G protein signaling over βarrestin2 recruitment in cell lines (26) to determine whether the

dopaminergic and behavioral outcomes can be segregated using a single ligand with divergent properties. We selected one compound from a collection previously described as a biased agonist at KOR on the basis of the following properties: it is representative of the degree of bias within the collection, it has efficacy in the warm water tail immersion assay, and it can enter the brain when administered systemically (26). We demonstrated that the bias properties in vitro were maintained when compared to a reference agonist (U50,488H) that is more suitable for in vivo evaluation. We showed that the compound triazole 1.1 [2-(4-(furan-2-ylmethyl)-5-((4-methyl-3-(trifluoromethyl)benzyl)thio)-4*H*-1,2,4-triazol-3-yl)pyridine] produced antinociception and had antipruritic properties in a dose-responsive manner, yet it did not decrease locomotor activity or dopamine release whether administered systemically or applied directly to brain slice preparations. Furthermore, our results demonstrate that a KOR agonist can alleviate pain without inducing dysphoria in a rat model of intracranial self-stimulation (ICSS).

RESULTS

Triazole 1.1 maintains G protein bias against U50,488H

We have previously reported that triazole 1.1 displays a preference for G protein signaling over βarrestin2 recruitment when compared to the reference agonist U69,593 (26). Here, we showed that the bias was maintained with the more brain-penetrant KOR agonist U50,488H, which was used for comparison in all of the behavioral models reported herein. As anticipated, U50,488H was a potent agonist for activating [^{35}S]-guanosine 5′-*O*-(3′-thiotriphosphate) ([^{35}S]GTPγS) binding and inducing βarrestin2 recruitment in cells expressing KOR and behaved similarly to U69,593 (Table 1) (30). The calculated bias factor (G protein/βarrestin2) of triazole 1.1 was 28 [95% confidence interval (CI), 19 to 40], indicating a substantial bias for inducing GTPγS binding over promoting βarrestin2 recruitment in these assays, compared to U50,488H (Table 1) (26, 31).

Triazole 1.1 causes antinociception and inhibits itch in mice

Triazole 1.1 induced antinociception in the warm water tail withdrawal (tail flick) assay that was comparable to that achieved with U50,488H (26), and further evaluation of the dose-response comparison demonstrated that although equivalent efficacy could be achieved, the efficacy of lower doses of triazole 1.1 was less than that observed for U50,488H (Fig. 1A). However, the responses induced by U50,488H did not differ in effect from those induced by triazole 1.1 (Fig. 1A). Norbinaltorphimine (NorBNI) fully antagonized the antinociception produced by both compounds (Fig. 1B). Neither drug had efficacy in KOR-KO mice (Fig. 1C), further demonstrating KOR selectivity in the antinociceptive actions of both compounds.

Triazole 1.1 was also efficacious in the mouse non-histamine pruritis model, which is produced by a subcutaneous injection of chloroquine phosphate at the base of the neck to induce robust scratching behaviors in mice. Triazole 1.1 suppressed chloroquine phosphate–induced scratching responses to a similar extent as did U50,488H (Fig. 1, D and E). All doses of both agonists significantly suppressed chloroquine phosphate–induced scratching, and U50,488H and triazole 1.1 did not significantly differ in effect from each other or from

vehicle + vehicle treatment at any dose tested (Fig. 1F). The antipruritic effects of KOR agonists can be blocked by a 24-hour pretreatment with NorBNI (8), and the effects of triazole 1.1 were fully antagonized by NorBNI (Fig. 1G).

Triazole 1.1 does not decrease locomotor activity in mice

Agonists of KOR decrease dopaminergic transmission and, as a result, produce sedative effects (10, 11, 32). In mice, this can be readily observed by a marked decrease in spontaneous ambulatory behaviors (8, 32). Therefore, we compared the two compounds for their abilities to modulate mouse activity in the open-field activity test. Upon treatment with U50,488H, ambulation was significantly suppressed within 10 min and persisted through the hour (Fig. 2A, left). Triazole 1.1 did not affect locomotor activity at any of the doses tested when compared to vehicle treatment (Fig. 2A, right). A comparison of the sum of activity for the duration of the test revealed a difference between the two agonists as a function of dose and treatment group (Fig. 2B). KOR-KO mice did not respond to U50,488H, suggesting that the actions of this drug were mediated through the KOR (Fig. 2C).

Triazole 1.1 occupies KOR in mouse striatum and can activate G protein signaling

Thus far, our data suggested that an agonist that promotes G protein signaling over βarrestin2 recruitment in cell culture studies could dissociate sedative behaviors from antinociceptive and antipruritic responses in mice. Conversely, it is possible that the different behaviors were mediated by KOR in physiologically distinct sites and that the two compounds could have pharmacokinetic differences that would prevent them from having equivalent exposure at those sites. KOR modulation of dopaminergic transmission is generally localized to presynaptic nerve terminals in the nucleus accumbens and striatum (33–35). We have previously demonstrated that triazole 1.1 is brain-penetrant by measuring tissue content in whole brain after systemic dosing (26). Here, we asked whether both compounds were present in striatum and occupied KOR at doses that produce different effects on locomotor activity. Thirty minutes after injection, U50,488H at 5 mg/kg suppressed locomotor activity to a similar extent as did U50,488H at 15 mg/kg (Fig. 3A); therefore, we chose this dose for comparison to triazole 1.1 at 15 mg/kg [a dose that produced no effect on locomotor activity (Fig. 2A)]. Using liquid chromatography–mass spectrometry (LC-MS) analysis of homogenized striatum, U50,488H and triazole 1.1 were detected at equivalent amounts 30 min after injection (Fig. 3B).

To activate KOR, the agonist must have access to the receptor in vivo. Therefore, we asked whether U50,488H or triazole 1.1 occupied striatal KOR and prevented subsequent radioligand binding. Thirty minutes treatment with either agonist reduced specific [^{3}H]U69,593 binding in striatum by 40% compared to untreated mice. Therefore, triazole 1.1 was present in striatum and occupied the [^{3}H]U69,593 binding site to a similar extent as did U50,488H (Fig. 3C) at doses at which U50,488H suppressed locomotor activity, whereas triazole 1.1 did not. To demonstrate that triazole 1.1 could activate KOR in striatum, we measured [^{35}S]GTPγS binding in striatal membranes and found that triazole 1.1 and U69,593 were similarly potent in activating G protein signaling (Fig. 3D). No significant [^{35}S]GTPγS binding was detected in KOR-KO mice for either agonist.

Triazole 1.1 does not decrease dopaminergic tone in mouse nucleus accumbens

Together, our data suggested that both U50,488H and triazole 1.1 had comparable opportunities to activate KOR in the striatum, yet triazole 1.1 did not affect locomotor activity in vivo, suggesting that it may not lead to decreases in dopaminergic tone. To directly test this hypothesis, we examined dopamine release by measuring electrically evoked dopamine concentrations using cyclic voltammetry in slice preparations containing the nucleus accumbens core and shell regions (Fig. 4, A and B). U50,488H produced a dose-dependent decrease in dopamine release in both regions. However, triazole 1.1 was markedly less potent and efficacious in this regard, inducing no measureable decreases in the core and a modest decrease in the shell only at the highest concentration tested.

Microdialysis sampling of nucleus accumbens was performed in freely moving mice after treatment to determine whether the neurochemical differences between compounds recapitulated the behavioral locomotor response. U50,488H treatment decreased dopamine concentration beyond 50% within the 2-hour test period, whereas triazole 1.1, even when tested at five times higher doses to assure occupancy, did not significantly affect dopamine concentrations (Fig. 4C). Together, these studies suggest that the G protein–biased KOR agonist triazole 1.1 maintained antinociceptive and antipruritic potency and efficacy without affecting dopaminergic transmission in mouse striatum.

Triazole 1.1 promotes analgesia in the absence of dysphoria in the rat ICSS model

To further address whether triazole 1.1 produces dysphoria-like effects, we opted to use the rat ICSS model, which is amenable to comparing compounds in a dose-responsive manner (36, 37). The aversive effects of KOR agonists are thought to be due to the inhibition of dopamine release in terminal fields in accumbens and striatum by KOR agonists because dopamine release from ascending fibers of passage through the medial forebrain bundle (MFB) is thought to largely mediate ICSS, as assessed by electrodes implanted into this region (36, 38, 39). In addition, acute pain stimuli will reduce ICSS supported by the MFB or ventral tegmental area (VTA), presumably at least in part through decreased dopaminergic tone (36, 37). In the ICSS assay, KOR agonists produce effects consistent with dysphoria and/or sedation in rats that are evidenced by shifts in either the threshold for ICSS or in frequency-rate curves (37–39).

Behaving as a typical KOR agonist, U50,488H shifted the frequency-response curve to the right (Fig. 5A) and increased the response threshold. The U50,488H-induced increases in EF_{50} (frequency required to generate half of the maximal ICSS response of the treatment) were dose-dependent compared to saline treatment, with the 6 mg/kg intraperitoneal dose being significantly different from saline (Fig. 5B, top). The effects of U50,488H on R_{max} (maximal ICSS response) were also dose-dependent, with 3 and 6 mg/kg shifting the frequency-response curve downward, that is, decreasing the top of the frequency-response curve compared to saline (Fig. 5B, bottom). The effects of the highest dose of U50,488H were blocked by pretreatment with NorBNI (Fig. 5, A and B). In contrast, triazole 1.1 did not alter either EF_{50} or R_{max} at doses up to 24 mg/kg compared to vehicle treatment (Fig. 5, C and D). Administration of either saline or triazole 1.1 vehicle did not significantly alter

either EF_{50} or R_{max} compared to baseline values (Fig. 5, A to D). LC-MS analysis of rat striata reveals that the two compounds were present after systemic injection (Fig. 5E).

Administration of lactic acid produced a significant rightward and downward shift in the frequency-rate curve for VTA ICSS that is indicative of its aversive effects due to irritation and pain at the intraperitoneal site of injection (Fig. 6) (36, 37). Accordingly, both the EF_{50} and R_{max} parameters were shifted after lactic acid injection compared to saline and baseline values (Fig. 6, A and B). As expected, treatment with the nonsteroidal anti-inflammatory drug ketoprofen before lactic acid injection completely blocked the effect of lactic acid as measured by changes in both EF_{50} and R_{max} (Fig. 6, A and B). Pretreatment with U50,488H did not reverse the effects of lactic acid on either EF_{50} or R_{max}, which were both significantly different from the values after saline pretreatment (Fig. 6, A and B). However, administration of triazole 1.1 suppressed the effect of lactic acid compared to vehicle administration (Fig. 6, C and D). The analgesic effect of triazole 1.1 was completely blocked by previous administration of NorBNI (Fig. 6, C and D), implicating a KOR-mediated effect. Neither saline nor triazole 1.1 vehicle affected the suppression of ICSS by lactic acid for either EF_{50} or R_{max} (Fig. 6, A to D).

DISCUSSION

This study detailed a small-molecule KOR agonist that displays biased agonism for G protein signaling over βarrestin2 recruitment in cell-based assays, which could induce antinociception and block pruritus without inducing sedation, decreasing dopamine concentrations, or producing behavioral indicators of dysphoria. These behavioral effects were fundamentally different from those induced by the conventional balanced agonist U50,488H, which produces antinociception and blocks itch yet also induces sedation, decreases dopamine concentrations, and produces dysphoria-like behaviors. We demonstrated that the effects of the compounds were mediated by KOR using antagonist blockade and KOR-KO mice. Furthermore, we demonstrated that the two compared compounds had equal opportunity to occupy the receptor in relevant sites of action (brain compared to periphery). Together, these data suggest that agonists that bias KOR signaling toward G protein over βarrestin2 recruitment in vitro may represent a new therapeutic strategy for capturing the desired analgesia and antipruritic effects of these drugs while eliminating sedative and dysphoric side effects.

There is substantial prior evidence to support that KOR-mediated antinociception is due to inhibitory G protein ($G\alpha_{i/o}$) signaling because pertussis toxin, which directly inhibits $G\alpha_{i/o}$ signaling, blocks KOR signaling in peripheral sensory neurons (40, 41). Furthermore, the antinociceptive properties of KOR agonists can be blocked by an intrathecal or intracerebroventricular injection of pertussis toxin (42–44). The antinociceptive properties of U69,593 are preserved in βarrestin2-KOmice, suggesting that βarrestin2 is not required for KOR-mediated antinociception (25). KOR agonists are also effective inhibitors of itch (5, 7, 8, 45). Notably, the relative potencies of KOR agonists have been correlated to their antinociceptive and antipruritic abilities in mice (46). Moreover, the antipruritic properties of U50,488H are preserved in βarrestin2-KO mice, suggesting that KOR agonists suppress itch by βarrestin2-independent signaling (8). The current study lends further evidence to suggest

that KOR agonists that display preferential functional affinity in promoting G protein coupling over βarrestin2 recruitment in vitro will maintain efficacy in rodent models of antinociception and pruritis.

In humans, KOR agonists negatively affect mood and cause sedation (15, 16, 47). In rodents, traditional KOR agonists lead to a decrease in spontaneous locomotor activity (48). KOR-mediated sedation has been associated with a decrease in dopaminergic transmission, and balanced KOR agonists such as U50,488H and U69,593 reduce dopamine concentrations in the nucleus accumbens (Fig. 4) (14, 49–51). However, triazole 1.1 did not elicit this response either on evoked dopamine release in brain slices measured by voltammetry or on basal concentrations of extracellular dopamine measured by microdialysis in freely moving mice (Fig. 4). Therefore, the current findings of relative neutrality of triazole 1.1 in locomotor activity assays are consistent with the association between decreased dopamine release and KOR-mediated sedation.

Decreases in dopamine release also promote dysphoria, which has been proposed as a mechanism by which KOR agonists produce aversive mood effects (14–16, 47, 49–51). Triazole 1.1 also did not cause any significant changes on ICSS when compared to baseline values or vehicle-treated rats (Figs. 5 and 6), yet it was efficacious in preventing the decreases in ICSS induced by lactic acid injection. The activity of triazole 1.1 in blocking acid-induced suppression of ICSS suggests a central site of action because peripherally restricted KOR agonists are inactive in this assay of pain behavior (52). One strength of this approach is that the same behavioral paradigm and endpoints are used to determine both dysphoria and antinociception in the same subjects. Together, these findings show separation in the neurophysiological effects of a G protein–biased KOR agonist in comparison to the reference ligand, indicating that the strategy of developing G protein–biased agonists at the KOR may be promising for developing novel pain treatment agents. These results complement the data obtained with mice and together show that, in contrast to U50,488H, triazole 1.1 did not cause aversion or sedation at doses that result in analgesia and antinociception.

It has been previously suggested that the KOR-mediated aversive and dysphoric properties are associated with the recruitment of βarrestin2 to the receptor (19, 41). Therefore, it is attractive to speculate that KOR-selective compounds that are biased against βarrestin2 recruitment (26) avoid inducing decreases in dopamine release and dysphoric effects due to the lack of βarrestin2 recruitment in vivo. However, it should be recognized that although this is an enticing hypothesis, the lack of βarrestin2 recruitment to the KOR has not been directly demonstrated in the mice. The identification of the precise neuronal populations that regulate such behaviors, as well as the refinement of tools needed to assess endogenous recruitment of βarrestin2, will facilitate such studies in the future. However, it remains possible that the lack of βarrestin2 recruitment in the cell-based assays simply indicates a change in receptor conformation and that changes in the receptor may result in a preference for a scaffold other than βarrestin2 in the endogenous setting.

We have described an isoquinolinone compound that displayed bias for G protein signaling (26) and that also induced antinociception and prevented itch at doses that did not decrease

locomotor activity (8). Furthermore, White *et al.* described a salvinorin A derivative, RB-64, that displays bias for G protein signaling over βarrestin2 recruitment and that preserves antinociceptive efficacy without decreasing locomotor activity (25). However, this natural product derivative produces conditioned place aversion (CPA) in mice (25). Although dopamine plays a critical role in place preference paradigms, dopamine deficient mice still display KOR-induced CPA, suggesting that there may be other mechanisms besides decreases in dopamine release at play in this model (53). KOR agonists can also cause psychotomimesis, hallucinations, and diuresis; however, the exact molecular mechanisms responsible for these properties are yet to be uncovered (15). The discovery of biased ligands with diverse signaling properties will provide additional tools for addressing these remaining questions.

The introduction of biased KOR agonists that have diverse chemical structure yet maintain similar bias profiles in cell-based assays and also produce similarly divergent behavioral responses will provide greater confidence that bias in vitro may be predictive of divergence of behaviors in vivo. Moreover, the development of these tools will also provide the opportunity to explore pathway-specific KOR-mediated effects in animal models. Caution must be taken in interpreting whether βarrestins are actually involved in mediating the adverse effects seen here as such direct demonstrations remain to be made. However, this work clearly demonstrates in vivo differences between a biased KOR agonist and the balanced agonist U50,488H, thus adding to the growing evidence that the analgesic properties can be separated from the sedative and dysphoric properties by altering how the agonist engages the KOR. Although more work to establish the cause of these effects is needed (and are underway), the present study represents an important correlation that may point a strategy to discover KOR agonists that can be advanced for the treatment of pain and itch.

MATERIALS AND METHODS

Chemicals and drugs

NorBNI and chloroquine phosphate were purchased from Sigma-Aldrich, and U50,488H was purchased from Tocris Bioscience. The synthesis of triazole 1.1 has been previously described (26). In most studies, U50,488H, NorBNI, and triazole 1.1 were prepared in a vehicle consisting of dimethyl sulfoxide (DMSO), Tween 80, and 0.9% sterile saline (1:1:8), with a pH of 6.0. Specifically, triazole 1.1 was first dissolved in DMSO and then in Tween 80 and brought up to volume with sterile saline; chloroquine phosphate was first dissolved in 0.9% sterile saline and brought up to volume with DMSO and Tween 80 to result in a 1:1:8 solution (pH6.0). DMSO, Tween 80, and lactic acid were obtained from Sigma-Aldrich. Chloroquine phosphate was freshly prepared and injected subcutaneously in the skin at the base of the neck (indicated by “sc neck”) at a volume of 5 μl/g body weight. Triazole 1.1 concentrations of 8 mg/ml or higher required heating the solution to boiling and then allowing it to cool to facilitate solubility. G protein coupling experiments and mass spectroscopy analysis were performed on the solution to assure that the compound integrity was maintained.

For the ICSS, voltammetry, and microdialysis studies, U50,488H and NorBNI were supplied as hydrochloride salts by the Drug Supply Program of the National Institute on Drug Abuse of the National Institutes of Health (Rockville, MD) and were dissolved in sterile water or 0.9% (w/v) NaCl, respectively. For rats, compounds were administered in a volume of 1 ml/kg. For mouse microdialysis studies, the components of the mobile phase, artificial cerebrospinal fluid (aCSF), and neurotransmitter standards were of high-performance liquid chromatography (HPLC) grade or the highest quality obtainable from Sigma-Aldrich.

Cell-based signaling assays for bias analysis

βarrestin2 recruitment assays were performed using the DiscoveRx PathHunter enzyme complementation assay (PathHunter U2OS OPRK1 β-Arrestin Cell Line) according to the manufacturer's instruction and as detailed previously (26). [^{35}S]GTPγS binding assays were performed on membranes prepared from CHO-K1 cells expressing a hemagglutinin-tagged human KOR as previously described (26). Data analyses were carried out using GraphPad Prism 6 (GraphPad Software) by applying three parameter, nonlinear regression analysis to the concentration-response curves for determining potency (EC_{50}) and efficacy (E_{max}) values. Test compounds were run in parallel with the reference compound (U50,488H), and all values were normalized to the E_{max} obtained with U50,488H and the baseline (unstimulated background) measures. The relative affinity transduction coefficients (Log$R$) and bias factors were calculated as previously described using the standard operational model as we have previously described (24, 31). In these calculations the ΔLogR of the test ligand was constrained to less than 10 and its affinity constant ($LogK_{test}$) was constrained to range from 1 fM to 1 M (24).

Animals

Male C57BL/6J mice were purchased from The Jackson Laboratory. KOR-KO mice were purchased from The Jackson Laboratory and propagated using homozygous breeding. Mice were group-housed (three to five mice per cage) and maintained on a 12-hour light/dark cycle in a temperature-controlled room. Adult mice between 10 and 14 weeks of age were used only once per assay. Dosing of mice was at 10 μl/g, sc or as specifically indicated in each experiment. The numbers of animals used in each assay are indicated in the figure legends. Because there are limits to the number of animals that could be assessed in each animal study at one time, vehicle and different doses of U50,488H and triazole 1.1 were tested in each group, resulting in more vehicle-treated animals than drug-treated groups. Power analysis was used to direct the size of the groups of animals per dose based on the responses observed in pilot studies as an attempt to minimize the numbers of animals used.

Seventeen male Fisher 344 rats (300 to 350 g, Harlan Sprague-Dawley) were individually housed in an AAALAC (Association for Assessment and Accreditation of Laboratory Animal Care)–approved, temperature- and humidity-controlled vivarium contained within the behavioral laboratory. Animals were kept on a 12-hour/12-hour reversed light/dark cycle (dark at 0500–1700 hours) and given ad libitum access to rat chow and water except during experimental sessions. All behavioral sessions occurred during the dark phase of the light/dark cycle. Additional male rats of the same age were obtained by the same vendor for drug

disposition studies conducted at The Scripps Research Institute. Dosing of rats was at 1 ml/kg, ip or as specifically indicated in each experiment.

Study approval

Experimental protocols applied to mice and rats adhered to National Institutes of Health Animal Care guidelines and were approved by The Scripps Research Institute (Jupiter, FL) and the Wake Forest School of Medicine (Winston-Salem, NC) Institutional Animal Care and Use Committees.

Warm water tail immersion (tail flick) assay

Antinociception was evaluated in the warm water tail immersion (tail flick) assay (49°C) as previously described (26). Briefly, ~2 cm of the tail was submersed in a warm water bath, and the time to withdrawal is recorded. A cutoff latency of 10 s was imposed to prevent tissue damage. Withdrawal latencies were recorded before (baseline) vehicle or drug administration and at 20 min after injection; the %MPE is calculated as follows: 100% × (response time − baseline / 10 s − baseline).

Pruritus

Mice were habituated to clear acrylic testing boxes (10 × 10 cm^2) for 1 hour before the start of the experiment. All mice received a pretreatment of either vehicle [DMSO, Tween 80, and 0.9% sterile saline (1:1:8)] or KOR agonists U50,488H or triazole 1.1 (5 μl/g, sc). Ten minutes after pretreatment, mice were injected with chloroquine phosphate (5 μl/g, sc neck) to induce acute pruritus. Immediately after the pruritogen injection, the number of scratching bouts was recorded every 5 min for 1 hour by an investigator blinded to the treatment groups. During the experiments, mice were videotaped, and for some studies, another investigator repeated scoring to validate the method. A “scratching bout” is defined as one or more rapid paw movements directed at the injection site, with the hindpaw being placed back on the floor as previously described (8, 54).

Locomotor activity

C57BL/6J male mice were monitored in an open-field activity monitor [Versamax (20 × 20 cm^2), Accuscan Instruments] immediately after injection with vehicle, U50,488H, or triazole 1.1 without habituation. Spontaneous activity was measured over 60 min, with the number of horizontal beam breaks collected in 5-min bins as previously described (8).

Pharmacokinetic and occupancy studies

Mice were killed by cervical dislocation, and rats were killed by carbon dioxide asphyxiation. Brains were collected, and striata were dissected 30 min after injection and immediately frozen in liquid nitrogen. The route of administration and dosing information are described in the figure legends. Compound concentrations in striatum samples were evaluated using LC (Shimadzu)–tandem mass spectrometry (AB Sciex) operated in positive-ion mode using multiple reaction monitoring methods (26). To determine occupancy, membrane preparations were made after tissue homogenization and subjected to radioligand binding assays as previously described (26). Briefly, homogenates were prepared in 10 mM

tris-HCl (pH 7.4), 100 mM NaCl, and 1 mM EDTA, and membrane pellets were collected without washing. Total binding was determined using [^{3}H]U69,593 (~2 nM, 43 Ci/mmol, PerkinElmer) in the presence of 10 μM cold U69,593 to determine nonspecific binding. After a 2-hour room temperature incubation, membranes (100 μg of protein for mouse and 300 μg of protein for rat) were collected on a 12-well Millipore vacuum harvester onto GFB filters soaked in 0.1% polyethyleneimine. Specific binding is calculated by subtracting nonspecific from total binding disintegrations per minute counts measured by scintillation counter.

Fast-scan cyclic voltammetry

In preparation for cyclic voltammetry studies, mice were killed by decapitation, and brains were rapidly removed and transferred into ice-cold, pre-oxygenated (95% O_2/5% CO_2) aCSF consisting of 126 mM NaCl, 2.5 mM KCl, 1.2 mM NaH_2PO_4, 2.4 mM $CaCl_2$, 1.2 mM $MgCl_2$, 25 mM $NaHCO_3$, 11 mM glucose, and 0.4 mM L-ascorbic acid, and pH was adjusted to 7.4. The brain was sectioned into 300-μm-thick coronal slices containing the striatum with a vibrating tissue slicer (Leica VT1000S, Vashaw Scientific) and transferred to a submersion recording chamber perfused at 1 ml/min at 32°C with oxygenated aCSF.

After an equilibration period (30 min), a carbon fiber microelectrode (length, ~150 μm; diameter, 7 μm) and a bipolar stimulating electrode were placed in close proximity to each other (about 100 μm apart) into the nucleus accumbens core. Dopamine was evoked by a single, rectangular, electrical pulse (300 μA, 2 ms) applied every 5 min. Extracellular dopamine was recorded every 100 ms using fast-scan cyclic voltammetry by applying a triangular waveform (−0.4 to +1.2 to −0.4 V versus Ag/AgCl, 400 V/s) (55). One slice was used per animal. After achieving a stable dopamine response, a cumulative concentration-response curve was obtained for U50,488H and triazole 1.1 (10, 30, 100, 300, and 1000 nM), with each dose added after signal stability was reached (about 30 min). Immediately after the completion of each experiment, recording electrodes were calibrated by recording their response [in current (expressed in nanoamperes)] to 3 μM dopamine in aCSF using a flow injection system.

To determine kinetic parameters, we modeled evoked levels of dopamine using Michaelis-Menten kinetics as a balance between release and uptake (56). Michaelis-Menten modeling of baseline dopamine signals provides parameters that describe the amount of dopamine released after stimulation and the maximal rate of dopamine uptake (V_{max}). For baseline modeling, we followed standard voltammetric modeling procedures by setting the apparent Michaelis constant (K_m) value to 160 nM for each animal based on well-established research on the affinity of dopamine for the dopamine transporter (57), whereas baseline V_{max} values were allowed to vary as the maximal rate of dopamine uptake. All voltammetry data were collected and modeled using Demon Voltammetry and Analysis Software (56).

Microdialysis

For microdialysis experiments, mice were anesthetized with a combination of ketamine (100 mg/kg, ip) and xylazine (10 mg/kg, ip). Guide cannulae (P000138; CMA Microdialysis, Harvard Apparatus) for probes were directed at the nucleus accumbens using the following

coordinates from bregma: anterior, +1.7 mm; lateral, −0.8 mm; and ventral, −3.0 mm (58). After a 24-hour recovery period, mice were placed in a microdialysis test chamber (CMA Microdialysis) housed within a sound-attenuating exterior chamber equipped with a light and fan. Microdialysis probes (P000082; CMA Microdialysis, Harvard Apparatus) were inserted into the cannula. A syringe containing aCSF [148 mM NaCl, 2.7 mM KCl, 1.2 mM $CaCl_2$, and 0.85 mM $MgCl_2$ (pH 7.4), with NaH_2PO_4] was placed in an infusion pump set to flow at a rate of 1.0 μl/min with at least a 2-hour period of equilibration before the start of the experiment. For all microdialysis experiments, samples (20 μl) were collected at 20-min intervals. Each sample was analyzed immediately by HPLC with electrochemical detection (ESA). All samples were analyzed using a mobile phase as described previously (59). Experiments commenced once a stable baseline was apparent (that is, three consecutive samples with consistent peaks). After the establishment of stable baselines, mice were injected with either U50,488H (3 mg/kg, ip) or triazole 1.1 (15 mg/kg, ip), and samples were collected for an additional 80 min. Immediately after the completion of the experiment, mice were killed by inhalation of isoflurane and cervical dislocation; brains were then removed for probe placement confirmation.

Intracranial self-stimulation

Rats were anesthetized with pentobarbital (50 mg/kg, ip) and atropine methyl nitrate (10 mg/kg, ip). After being placed in a stereotaxic frame, platinum bipolar stimulating electrodes (Plastics One) were implanted into the left VTA (2.3 mm anterior to lambda, 0.6 mm lateral from the midline, and 8.5 mm below the skull surface). Three stainless steel screws embedded in dental acrylic permanently secured each electrode to the skull surface. After implantation, rats received penicillin G procaine (75,000 U, intramuscularly) to prevent infection.

An operant chamber with a lever 5 cm above a grid bar floor, a stimulus lamp 2 cm above the lever, and a tone generator were used (Med Associates Inc.). The operant chamber was housed within a sound- and light-attenuating enclosure containing a houselight and a ventilation fan. An ICSS stimulator controlled by a computer software program (Med Associates Inc.) that controlled all stimulation parameters and data collection was located outside the enclosure. A two-channel swivel commutator (model SLC2C, Plastics One) located above the operant chamber connected the electrodes to the ICSS stimulator via 25-cm cables (Plastics One).

After at least 14 days of recovery from surgery, rats were trained to lever press for brain stimulation. A stimulus light located above the lever indicated stimulation availability. Lever presses produced a 0.5-s train of rectangular alternating cathodal and anodal pulses (0.1-ms pulse durations); stimulation was also accompanied by the stimulus light turning off, the illumination of the houselight, and the sound of a tone. Additional responses during the 0.5-s stimulation period resulted in no further stimulation and were not recorded.

During initial acquisition sessions, the frequency was held constant (156 Hz) and the intensity was adjusted by the experimenter to determine the lowest intensity that maintained high rates of responding (>40 responses/min). Once responding was established, frequency-

rate curves were generated. These 2-hour sessions consisted of six 10-min components, which were further broken down into ten 1-min trials.

Each 60-s trial consisted of a 5-s timeout, followed by a 5-s period during which five noncontingent stimulations were delivered, and then a 50-s period during which lever presses resulted in stimulation and were recorded. During these sessions, the intensity remained constant (unique to each animal), and a series of 10 frequencies (156 to 45 Hz, 0.06 log increments corresponding to each trial) were presented in descending order. A 1-hour timeout period between components 3 and 4 permitted drug injections during test sessions.

U50,488H was injected subcutaneously in a volume of 1 ml/kg 30 min before ICSS component 4 began. Triazole 1.1 was injected in a volume of 1, 2, or 3 ml/kg to achieve final doses of 8, 16, or 24 mg/kg, sc, respectively. The 4 mg/kg dose of triazole 1.1 was achieved by diluting the 8 mg/ml solution with vehicle (1:1) and injecting in a volume of 1 ml/kg, sc. For pharmacological comparisons, vehicle injections were in a volume of 3 ml/kg, sc. Triazole 1.1 or vehicle was injected subcutaneously 45 min before component 4 of the ICSS session began. Animals were injected with NorBNI (32 mg/kg, sc) 24 hours before ICSS sessions, and animals were injected with U50,488H (6 mg/kg, sc) 48 hours after NorBNI. Triazole 1.1 (24 mg/kg, sc) and 1.8% lactic acid were administered 72 hours after NorBNI administration with pretreatment times the same as described above for each drug. After ICSS studies, rats were killed by carbon dioxide asphyxiation to prepare samples for histology. Brains were rapidly removed and frozen in isopentane (−35°C) and were stored at −80°C. Coronal sections (25 μm) around the electrode tract were obtained using a cryostat to confirm electrode placement within the VTA.

Frequency-rate curves were averaged for the two components preceding drug injection (components 2 and 3) and separately for the three components after drug injection (components 4, 5, and 6); these averaged frequency-rate curves were fit to a sigmoidal dose-response function with variable slope using GraphPad Prism 6 software as described previously for each individual session and for each subject (60). The frequency that resulted in the half-maximal response rate (EF_{50}) and the maximal response rate (R_{max}) were determined before and after injections separately. The effect of drug treatment on VTA ICSS was analyzed using one-way ANOVA with drug dose serving as the independent variable and ΔEF_{50} (EF_{50} before injection − EF_{50} after injection) or ΔR_{max} (R_{max} before injection − R_{max} after injection) serving as the dependent measures. ΔEF_{50} and ΔR_{max} were compared between treatments using one-way ANOVA, and planned post hoc comparisons were made using a Bonferroni *t* test using GraphPad Prism 6 (60).

General statistics

All statistical comparisons were made using GraphPad Prism 6 software and are expressed as means ± SEM. Differences between means were analyzed using one-way ANOVA for comparisons within the same genotype and by two-way ANOVA for comparisons between genotypes and time-course evaluation. All ANOVAs were followed with Bonferroni post hoc analysis, and in all analyses, significance was set at $P < 0.05$.

Acknowledgments

Funding: This work was supported by NIH grants P01GM113852 and P50DA006634 (to T.J.M.), R01DA014030 and U01AA014091 (to S.R.J.), and R01DA031297 (to L.M.B. and J.A.).

Triazole 1.1 is included in the U.S. patent US 9,345, 703 B2, May 24, 2016.

REFERENCES AND NOTES

1. Zhou L, Stahl EL, Lovell KM, Frankowski KJ, Prisinzano TE, Aubé J, Bohn LM. Characterization of kappa opioid receptor mediated, dynorphin-stimulated [^{35}S]GTPγS binding in mouse striatum for the evaluation of selective KOR ligands in an endogenous setting. Neuropharmacology. 2015; 99:131–141. [PubMed: 26160155]
2. Chavkin C, James IF, Goldstein A. Dynorphin is a specific endogenous ligand of the kappa opioid receptor. Science. 1982; 215:413–415. [PubMed: 6120570]
3. Mansour A, Khachaturian H, Lewis ME, Akil H, Watson SJ. Anatomy of CNS opioid receptors. Trends Neurosci. 1988; 11:308–314. [PubMed: 2465635]
4. Kivell B, Prisinzano TE. Kappa opioids and the modulation of pain. Psychopharmacology (Berl). 2010; 210:109–119. [PubMed: 20372880]
5. Cowan A, Kehner GB, Inan S. Targeting itch with ligands selective for κ opioid receptors. Handb. Exp. Pharmacol. 2015; 226:291–314. [PubMed: 25861786]
6. Inan S, Cowan A. Kappa opioid agonists suppress chloroquine-induced scratching in mice. Eur. J. Pharmacol. 2004; 502:233–237. [PubMed: 15476749]
7. Kardon AP, Polgar E, Hachisuka J, Snyder LM, Cameron D, Savage S, Cai X, Karnup S, Fan CR, Hemenway GM, Bernard CS, Schwartz ES, Nagase H, Schwarzer C, Watanabe M, Furuta T, Kaneko T, Koerber HR, Todd AJ, Ross SE. Dynorphin acts as a neuromodulator to inhibit itch in the dorsal horn of the spinal cord. Neuron. 2014; 82:573–586. [PubMed: 24726382]
8. Morgenweck J, Frankowski KJ, Prisinzano TE, Aubé J, Bohn LM. Investigation of the role of βarrestin2 in kappa opioid receptor modulation in a mouse model of pruritus. Neuropharmacology. 2015; 99:600–609. [PubMed: 26318102]
9. Kumagai H, Ebata T, Takamori K, Muramatsu T, Nakamoto H, Suzuki H. Effect of a novel kappa-receptor agonist, nalfurafine hydrochloride, on severe itch in 337 haemodialysis patients: A phase III, randomized, double-blind, placebo-controlled study. Nephrol. Dial. Transplant. 2010; 25:1251–1257. [PubMed: 19926718]
10. Bruijnzeel AW. kappa-Opioid receptor signaling and brain reward function. Brain Res. Rev. 2009; 62:127–146. [PubMed: 19804796]
11. Chefer VI, Czyzyk T, Bolan EA, Moron J, Pintar JE, Shippenberg TS. Endogenous κ-opioid receptor systems regulate mesoaccumbal dopamine dynamics and vulnerability to cocaine. J. Neurosci. 2005; 25:5029–5037. [PubMed: 15901784]
12. Shippenberg TS, Chefer VI, Zapata A, Heidbreder CA. Modulation of the behavioral and neurochemical effects of psychostimulants by κ-opioid receptor systems. Ann. N. Y. Acad. Sci. 2001; 937:50–73. [PubMed: 11458540]
13. Karkhanis AN, Rose JH, Weiner JL, Jones SR. Early-life social isolation stress increases kappa opioid receptor responsiveness and downregulates the dopamine system. Neuropsychopharmacology. 2016; 41:2263–2274. [PubMed: 26860203]
14. Rose JH, Karkhanis AN, Chen R, Gioia D, Lopez MF, Becker HC, McCool BA, Jones SR. Supersensitive kappa opioid receptors promotes ethanol withdrawal-related behaviors and reduce dopamine signaling in the nucleus accumbens. Int. J. Neuropsychopharmacol. 2016; 19:pyv127. [PubMed: 26625893]
15. Pfeiffer A, Brantl V, Herz A, Emrich HM. Psychotomimesis mediated by kappa opiate receptors. Science. 1986; 233:774–776. [PubMed: 3016896]
16. Knoll AT, Carlezon WA Jr. Dynorphin, stress, and depression. Brain Res. 2010; 1314:56–73. [PubMed: 19782055]

17. Werling LL, Frattali A, Portoghese PS, Takemori AE, Cox BM. Kappa receptor regulation of dopamine release from striatum and cortex of rats and guinea pigs. J. Pharmacol. Exp. Ther. 1988; 246:282–286. [PubMed: 2839666]
18. Crowley NA, Kash TL. Kappa opioid receptor signaling in the brain: Circuitry and implications for treatment. Prog. Neuropsychopharmacol. Biol. Psychiatry. 2015; 62:51–60. [PubMed: 25592680]
19. Bruchas MR, Land BB, Aita M, Xu M, Barot SK, Li S, Chavkin C. Stress-induced p38 mitogen-activated protein kinase activation mediates κ-opioid-dependent dysphoria. J. Neurosci. 2007; 27:11614–11623. [PubMed: 17959804]
20. Cahill CM, Taylor AM, Cook C, Ong E, Moron JA, Evans CJ. Does the kappa opioid receptor system contribute to pain aversion? Front. Pharmacol. 2014; 5:253. [PubMed: 25452729]
21. Wittmann W, Schunk E, Rosskothen I, Gaburro S, Singewald N, Herzog H, Schwarzer C. Prodynorphin-derived peptides are critical modulators of anxiety and regulate neurochemistry and corticosterone. Neuropsychopharmacology. 2009; 34:775–785. [PubMed: 18800067]
22. Rankovic Z, Brust TF, Bohn LM. Biased agonism: An emerging paradigm in GPCR drug discovery. Bioorg. Med. Chem. Lett. 2016; 26:241–250. [PubMed: 26707396]
23. Bruchas MR, Macey TA, Lowe JD, Chavkin C. Kappa opioid receptor activation of p38 MAPK is GRK3- and arrestin-dependent in neurons and astrocytes. J. Biol. Chem. 2006; 281:18081–18089. [PubMed: 16648139]
24. Lovell KM, Frankowski KJ, Stahl EL, Slauson SR, Yoo E, Prisinzano TE, Aubé J, Bohn LM. Structure-activity relationship studies of functionally selective kappa opioid receptor agonists that modulate ERK 1/2 phosphorylation while preserving G protein over βarrestin2 signaling bias. ACS Chem. Neurosci. 2015; 6:1411–1419. [PubMed: 25891774]
25. White KL, Robinson JE, Zhu H, DiBerto JF, Polepally PR, Zjawiony JK, Nichols DE, Malanga CJ, Roth BL. The G protein–biased κ-opioid receptor agonist RB-64 is analgesic with a unique spectrum of activities in vivo. J. Pharmacol. Exp. Ther. 2015; 352:98–109. [PubMed: 25320048]
26. Zhou L, Lovell KM, Frankowski KJ, Slauson SR, Phillips AM, Streicher JM, Stahl E, Schmid CL, Hodder P, Madoux F, Cameron MD, Prisinzano TE, Aubé J, Bohn LM. Development of functionally selective, small molecule agonists at kappa opioid receptors. J. Biol. Chem. 2013; 288:36703–36716. [PubMed: 24187130]
27. Brust TF, Hayes MP, Roman DL, Watts VJ. New functional activity of aripiprazole revealed: Robust antagonism of D2 dopamine receptor-stimulated Gβγ signaling. Biochem. Pharmacol. 2015; 93:85–91. [PubMed: 25449598]
28. Shenoy SK, Lefkowitz RJ. β-arrestin-mediated receptor trafficking and signal transduction. Trends Pharmacol. Sci. 2011; 32:521–533. [PubMed: 21680031]
29. Lefkowitz RJ, Shenoy S. Transduction of receptor signals by β-arrestins. Science. 2005; 308:512–517. [PubMed: 15845844]
30. Von Voigtlander PF, Lewis RA. U-50,488, a selective kappa opioid agonist: Comparison to other reputed kappa agonists. Prog. Neuropsychopharmacol. Biol. Psychiatry. 1982; 6:467–470. [PubMed: 6298890]
31. Stahl EL, Zhou L, Ehlert FJ, Bohn LM. A novel method for analyzing extremely biased agonism at G protein–coupled receptors. Mol. Pharmacol. 2015; 87:866–877. [PubMed: 25680753]
32. Von Voigtlander PF, Lahti RA, Ludens JH. U-50,488: A selective and structurally novel non-Mu (kappa) opioid agonist. J. Pharmacol. Exp. Ther. 1983; 224:7–12. [PubMed: 6129321]
33. Di Chiara G, Imperato A. Opposite effects of mu and kappa opiate agonists on dopamine release in the nucleus accumbens and in the dorsal caudate of freely moving rats. J. Pharmacol. Exp. Ther. 1988; 244:1067–1080. [PubMed: 2855239]
34. Ronken E, Mulder AH, Schoffelmeer AN. Interacting presynaptic κ-opioid and $GABA_A$ receptors modulate dopamine release from rat striatal synaptosomes. J. Neurochem. 1993; 61:1634–1639. [PubMed: 8228982]
35. Svingos AL, Colago EE, Pickel VM. Cellular sites for dynorphin activation of κ-opioid receptors in the rat nucleus accumbens shell. J. Neurosci. 1999; 19:1804–1813. [PubMed: 10024364]
36. Negus SS, Miller LL. Intracranial self-stimulation to evaluate abuse potential of drugs. Pharmacol. Rev. 2014; 66:869–917. [PubMed: 24973197]

37. Negus SS, Morrissey EM, Rosenberg M, Cheng K, Rice KC. Effects of kappa opioids in an assay of pain-depressed intracranial self-stimulation in rats. Psychopharmacology (Berl). 2010; 210:149–159. [PubMed: 20101391]
38. Todtenkopf MS, Marcus JF, Portoghese PS, Carlezon WA Jr. Effects of κ-opioid receptor ligands on intracranial self-stimulation in rats. Psychopharmacology (Berl). 2004; 172:463–470. [PubMed: 14727002]
39. Carlezon WA Jr, Béguin C, DiNieri JA, Baumann MH, Richards MR, Todtenkopf MS, Rothman RB, Ma Z, Lee DY-W, Cohen BM. Depressive-like effects of the κ-opioid receptor agonist salvinorin A on behavior and neurochemistry in rats. J. Pharmacol. Exp. Ther. 2006; 316:440–447. [PubMed: 16223871]
40. Berg KA, Rowan MP, Sanchez TA, Silva M, Patwardhan AM, Milam SB, Hargreaves KM, Clarke WP. Regulation of κ-opioid receptor signaling in peripheral sensory neurons in vitro and in vivo. J. Pharmacol. Exp. Ther. 2011; 338:92–99. [PubMed: 21487072]
41. Chavkin C. The therapeutic potential of κ-opioids for treatment of pain and addiction. Neuropsychopharmacology. 2011; 36:369–370. [PubMed: 21116263]
42. Goicoechea C, Ormazábal MJ, Abalo R, Alfaro MJ, Martín MI. Calcitonin reverts pertussis toxin blockade of the opioid analgesia in mice. Neurosci. Lett. 1999; 273:175–178. [PubMed: 10515187]
43. Przewlocki R, Costa T, Lang J, Herz A. Pertussis toxin abolishes the antinociception mediated by opioid receptors in rat spinal cord. Eur. J. Pharmacol. 1987; 144:91–95. [PubMed: 2830121]
44. Hernandez A, Soto-Moyano R, Mestre C, Eschalier A, Pelissier T, Paeile C, Contreras E. Intrathecal pertussis toxin but not cyclic AMP blocks kappa opioid-induced antinociception in rat. Int. J. Neurosci. 1995; 81:193–197. [PubMed: 7628910]
45. Togashi Y, Umeuchi H, Okano K, Ando N, Yoshizawa Y, Honda T, Kawamura K, Endoh T, Utsumi J, Kamei J, Tanaka T, Nagase H. Antipruritic activity of the κ-opioid receptor agonist, TRK-820. Eur. J. Pharmacol. 2002; 435:259–264. [PubMed: 11821035]
46. Wang Y, Tang K, Inan S, Siebert D, Holzgrabe U, Lee DY, Huang P, Li JG, Cowan A, Liu-Chen LY. Comparison of pharmacological activities of three distinct κ ligands (Salvinorin A, TRK-820 and 3FLB) on κ opioid receptors in vitro and their antipruritic and antinociceptive activities in vivo. J. Pharmacol. Exp. Ther. 2005; 312:220–230. [PubMed: 15383632]
47. Barber A, Gottschlich R. Novel developments with selective, non-peptidic kappa-opioid receptor agonists. Expert Opin. Investig. Drugs. 1997; 6:1351–1368.
48. Kunihara M, Ohyama M, Nakano M. Effects of spiradoline mesylate, a selective κ-opioid-receptor agonist, on the central dopamine system with relation to mouse locomotor activity and analgesia. Jpn. J. Pharmacol. 1993; 62:223–230. [PubMed: 8411771]
49. Hoffman AF, Spivak CE, Lupica CR. Enhanced dopamine release by dopamine transport inhibitors described by a restricted diffusion model and fast-scan cyclic voltammetry. ACS Chem. Neurosci. 2016; 7:700–709. [PubMed: 27018734]
50. Schoffelmeer AN, Hogenboom F, Mulder AH. κ_1- and κ_2-opioid receptors mediating presynaptic inhibition of dopamine and acetylcholine release in rat neostriatum. Br. J. Pharmacol. 1997; 122:520–524. [PubMed: 9351509]
51. Xi Z-X, Fuller SA, Stein EA. Dopamine release in the nucleus accumbens during heroin self-administration is modulated by kappa opioid receptors: An in vivo fast-cyclic voltammetry study. J. Pharmacol. Exp. Ther. 1998; 284:151–161. [PubMed: 9435173]
52. Negus SS, O'Connell R, Morrissey E, Cheng K, Rice KC. Effects of peripherally restricted κ opioid receptor agonists on pain-related stimulation and depression of behavior in rats. J. Pharmacol. Exp. Ther. 2012; 340:501–509. [PubMed: 22128346]
53. Land BB, Bruchas MR, Schattauer S, Giardino WJ, Aita M, Messinger D, Hnasko TS, Palmiter RD, Chavkin C. Activation of the kappa opioid receptor in the dorsal raphe nucleus mediates the aversive effects of stress and reinstates drug seeking. Proc. Natl. Acad. Sci. U.S.A. 2009; 106:19168–19173. [PubMed: 19864633]
54. Holmes FE, Vanderplank P, Wynick D. Galanin-expression and galanin-dependent sensory neurons are not required for itch. Mol. Pain. 2012; 8:87. [PubMed: 23216829]

55. Calipari ES, Ferris MJ, Melchior JR, Bermejo K, Salahpour A, Roberts DC, Jones SR. Methylphenidate and cocaine self-administration produce distinct dopamine terminal alterations. Addict. Biol. 2014; 19:145–155. [PubMed: 22458761]

56. Yorgason JT, España RA, Jones SR. Demon voltammetry and analysis software: Analysis of cocaine-induced alterations in dopamine signaling using multiple kinetic measures. J. Neurosci. Methods. 2011; 202:158–164. [PubMed: 21392532]

57. Wu Q, Reith ME, Wightman RM, Kawagoe KT, Garris PA. Determination of release and uptake parameters from electrically evoked dopamine dynamics measured by real-time voltammetry. J. Neurosci. Methods. 2001; 112:119–133. [PubMed: 11716947]

58. Paxinos, G.; Watson, C. The Rat Brain in Stereotaxic Coordinates. 6. Academic Press; 2007.

59. Karkhanis AN, Locke JL, McCool BA, Weiner JL, Jones SR. Social isolation rearing increases nucleus accumbens dopamine and norepinephrine responses to acute ethanol in adulthood. Alcohol. Clin. Exp. Res. 2014; 38:2770–2779. [PubMed: 25421514]

60. Ewan EE, Martin TJ. Opioid facilitation of rewarding electrical brain stimulation is suppressed in rats with neuropathic pain. Anesthesiology. 2011; 114:624–632. [PubMed: 21293250]

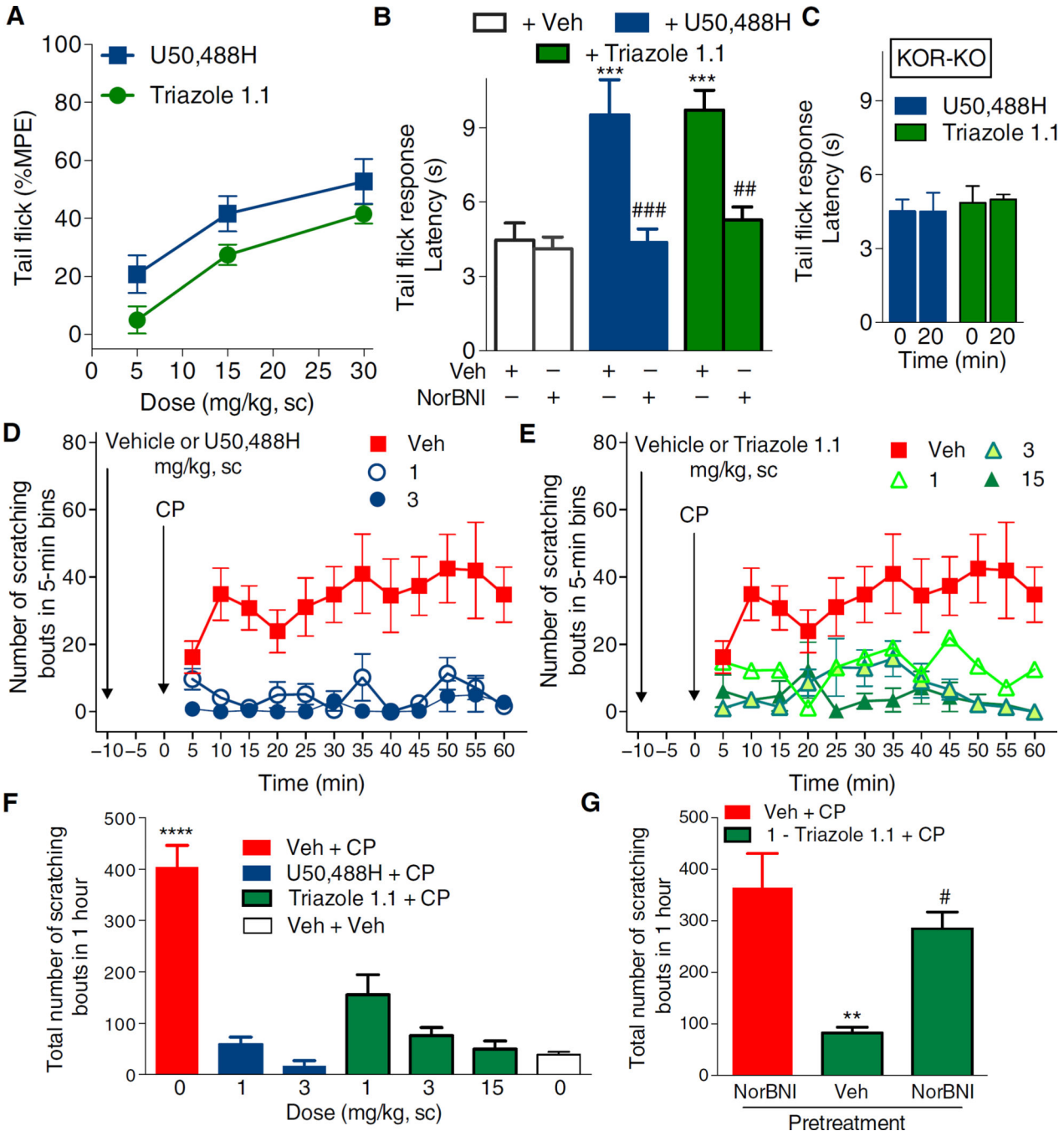

Fig. 1. Triazole 1.1 induces KOR-mediated antinociception and suppresses chloroquine phosphate–induced scratching responses in C57BL/6 mice

(**A**) U50,488H or triazole 1.1 produced an increase in response latency in a dose-dependent manner in the warm water tail flick assay (49°C). A 10-s cutoff was imposed to calculate the %MPE (maximum possible effect). For this group, the average baseline response was 2.7 ± 0.1 s. For dose effect: $F_{2,48} = 19.11$, $P < 0.0001$; for drug comparison: $F_{1,48} = 9.054$, $P = 0.0042$; Bonferroni post hoc comparison of the means at each dose indicated no differences ($P > 0.05$), $n = 7$ to 11 mice per treatment. sc, subcutaneous. (**B**) NorBNI [15 mg/kg,

intraperitoneally (ip), 10 min before agonist] prevented both U50,488H- and triazole 1.1–induced antinociception in the tail flick test. ***$P < 0.001$ compared to vehicle (Veh) + Veh; ###$P < 0.001$, ##$P < 0.01$ compared to respective agonist alone, one-way analysis of variance (ANOVA), Bonferroni post hoc analysis. For this group, the average baseline response was 4.2 ± 0.2 s; $n = 5$ to 7 mice per treatment. (**C**) Neither U50,488H nor triazole 1.1 (30 mg/kg, ip) delayed response latencies in KOR-KO (knockout) mice. The average baseline response was 4.7 ± 0.2 s. $n = 4$ KOR-KO mice per treatment. (**D** and **E**) U50,488H (D) (dose effect: $F_{2,204} = 71.67$, $P < 0.0001$) and triazole 1.1 (E) (dose effect: $F_{3,252} = 44.57$, $P < 0.0001$) dose-dependently suppressed scratching in response to chloroquine phosphate (CP) (40 mg/kg, sc neck) in C57BL/6 mice when administered 10 min before chloroquine phosphate challenge. Two-way ANOVA for dose effect in (A) and (B), $P < 0.0001$. (**F**) Total number of scratching bouts over the 1-hour period. U50,488H and triazole 1.1 significantly suppressed the scratching response at all doses tested (****$P < 0.0001$, one-way ANOVA). Triazole 1.1 and U50,488H did not significantly differ at each dose or from “veh + veh”–treated mice ($P > 0.05$). (**G**) NorBNI (10 mg/kg, ip, 24 hours prior) blocked the antipruritic effects of triazole 1.1 (1 mg/kg, sc). **$P < 0.01$ compared to NorBNI + CP; #$P < 0.05$ compared to triazole 1.1 + CP, one-way ANOVA. Data are means ± SEM; $n = 5$ to 9 C57BL/6 mice per dose for (D) to (G).

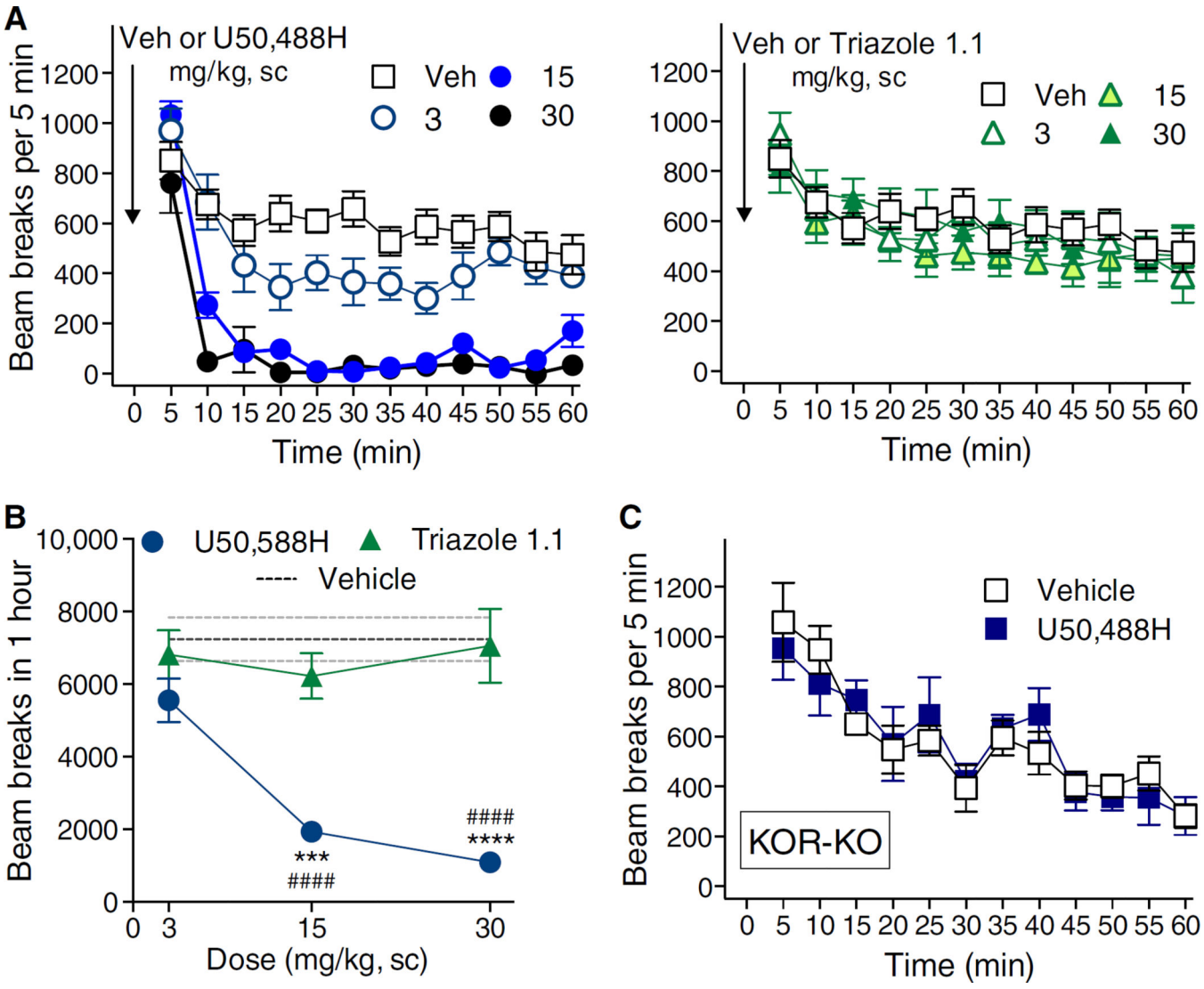

Fig. 2. Triazole 1.1 does not affect ambulatory behaviors in mice

(**A**) U50,488H (left) dose-dependently decreased locomotor activity over time (two-way ANOVA for dose, $P < 0.0001$), whereas triazole 1.1 (right) has no effect ($P > 0.05$). $n = 4$ to 11 mice per dose and treatment. (**B**) The total number of beam breaks observed in 1 hour significantly differed between U50,488H and triazole 1.1 treatment. Two-way ANOVA for interaction of dose and treatment: $F_{2,28} = 12.54$, $P = 0.0083$; Bonferroni post hoc analysis: $^{***}P < 0.001$, $^{****}P < 0.0001$ compared to triazole 1.1; U50,488H effects significantly differed from vehicle (interaction of dose and treatment: $F_{1,44} = 66.86$, $P < 0.0001$; Bonferroni post hoc analysis: $^{\#\#\#\#}P < 0.0001$ compared to vehicle). $n = 4$ to 11 mice per dose and treatment. (**C**) KOR-KO mice did not differ in their responses to U50,488H (30 mg/kg, sc) and vehicle whether analyzed over time or as the summation of activity over the hour (two-way ANOVA for drug effect: $P < 0.05$, $n = 4$ to 7 mice per treatment). Data are means ± SEM.

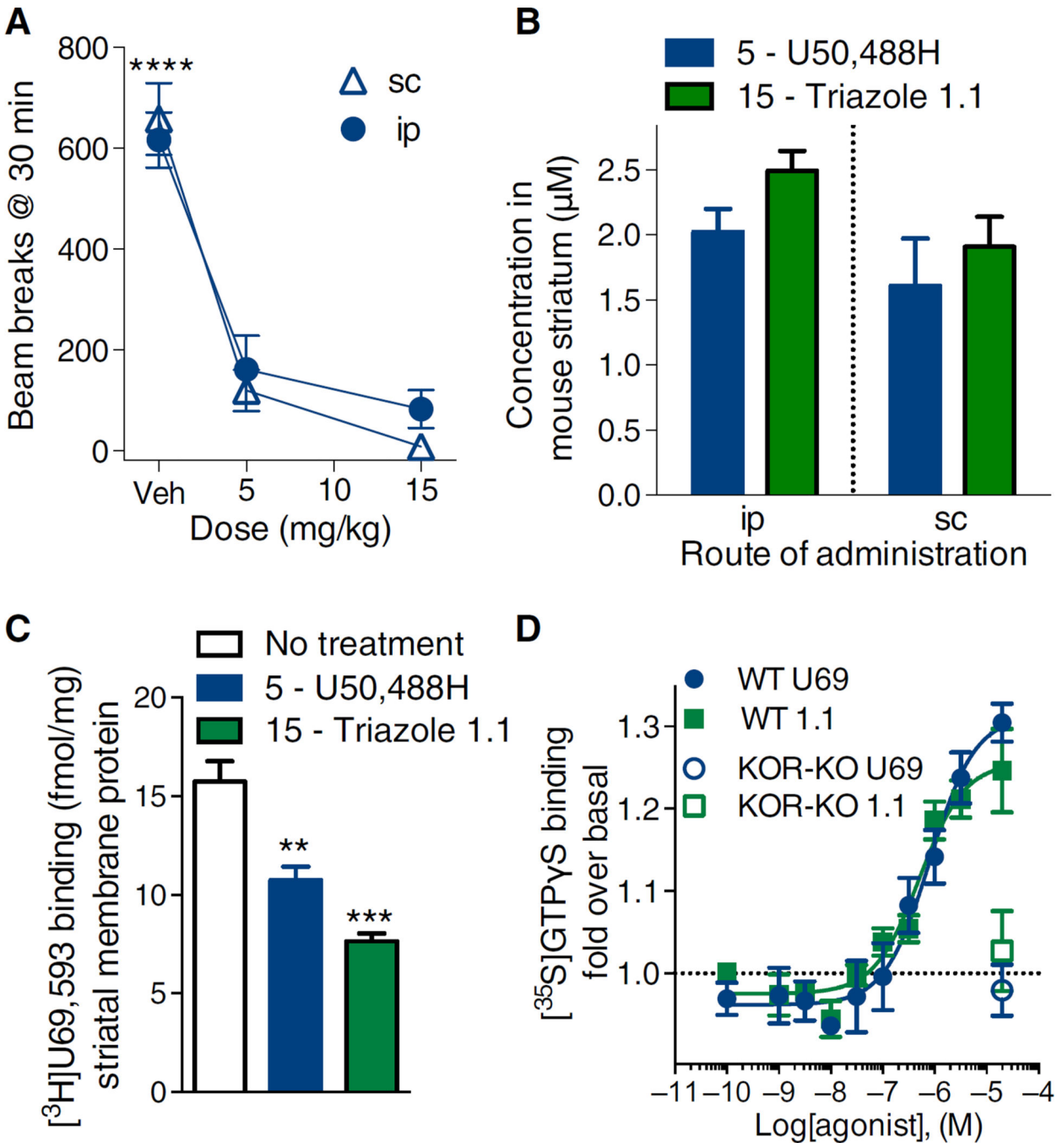

Fig. 3. Triazole 1.1 and U50,488H are present in striatum at comparable amounts where they activate KOR-mediated G protein signaling in striatum

(**A**) U50,488H suppressed activity to a similar extent at 5 and 15 mg/kg (ip or sc) at the 30-min time point (**** $P < 0.0001$ compared to 5 and 15 mg/kg compared within route of administration, two-way ANOVA). The 5 and 15 mg/kg doses did not differ ($P > 0.05$). $n = 5$ to 11 mice per dose and administration method. (**B**) Compound amounts detected in mouse striatum 30 min after injection are similar regardless of route of administration (ip or sc). The systemically administered 5 mg/kg dose of U50,488H resulted in equivalent distribution

as the 15 mg/kg dose of triazole 1.1. $P > 0.05$. $n = 3$ to 4 mice per treatment and administration method. (**C**) Intraperitoneal injection of agonist reduced the amount of [^{3}H]U69,593 binding that was detected compared to striatum taken from untreated mice (**$P < 0.01$, ***$P < 0.0001$ compared to no treatment group, one-way ANOVA). $n = 3$ to 6 independent experiments. (**D**) Triazole 1.1 activates G protein coupling that did not significantly differ from the effects of the KOR-selective agonist U69,593 in the mouse striatum (U69,593: $EC_{50} = 620 \pm 169$ nM; triazole 1.1: $EC_{50} = 497 \pm 34$ nM, $P > 0.05$). $n =$ 3 to 7 independent experiments. WT, wild type.

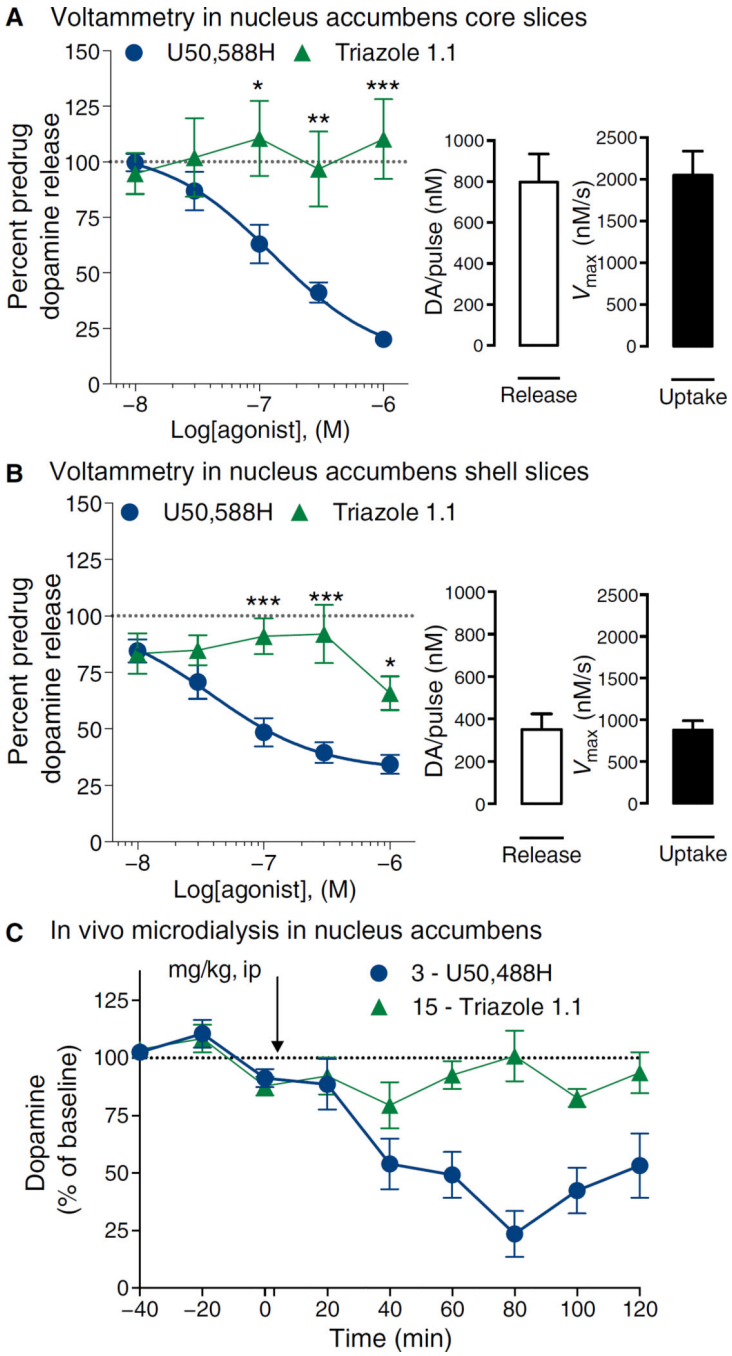

Fig. 4. U50,488H but not triazole 1.1 decreases dopamine concentrations in the nucleus accumbens in mice

(**A** and **B**) Cyclic voltammetric measures of dopamine release were made in slices of mouse brain in the nucleus accumbens. Triazole 1.1 did not induce decreases in dopamine release (nonconvergence of curves), whereas U50,488H did in a dose-dependent manner in both the core (A) [EC_{50} = 129 nM (95% CI, 51 to 230)] and the shell of the nucleus accumbens (B) [EC_{50} = 38 nM (95% CI, 9 to 157)]. Two-way ANOVA for dose and drug interaction: P = 0.0009; Bonferroni post hoc analysis: *P < 0.05, **P < 0.01, ***P < 0.001. The basal

concentrations of dopamine (DA) release and rate of clearance are provided for each section in the bar charts. Data are means ± SEM of six to seven mice per treatment. (**C**) Microdialysis in nucleus accumbens of freely moving mice confirms a decrease in dopamine in response to U50,488H (3 mg/kg, ip), whereas triazole 1.1 (15 mg/kg, ip) did not decrease the baseline and was significantly different from U50,488H ($P < 0.05$, two-way ANOVA). $n = 6$ to 7 mice per treatment.

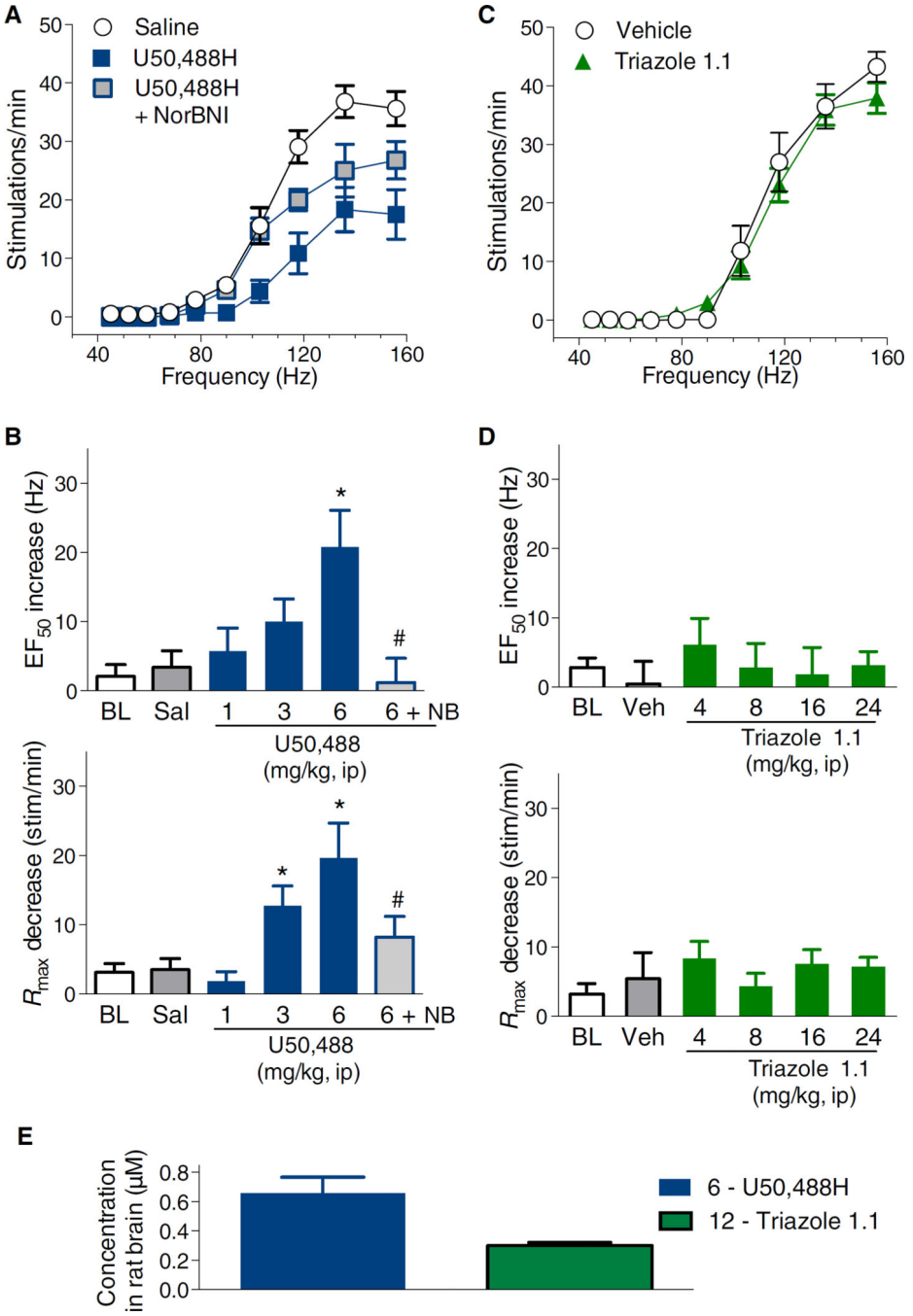

Fig. 5. U50,488H but not triazole 1.1 suppresses VTA ICSS in rats

(**A**) U50,488H (6 mg/kg, ip) suppressed VTA ICSS in a NorBNI (NB, 32 mg/kg, ip, 24 hours prior) reversible manner. (**B**) Dose-response effects on shifts in frequency (EF_{50}) and maximal responses (R_{max}) from frequency-rate curves are shown. The effects of U50,488H on EF_{50} ($F_{3,51} = 4.3$, $P = 0.009$) and R_{max} ($F_{3,51} = 7.2$, $P = 0.0004$) are dose-dependent compared to saline treatment. One-way ANOVA for drug effect for EF_{50} (top) indicates $^{*}P < 0.05$ compared to saline (Sal); $^{\#}P < 0.05$ compared to U50,488H (6 mg/kg, ip). One-way ANOVA for R_{max} (bottom) indicates $P < 0.05$ compared to saline and $^{\#}P < 0.05$ compared to

U50,488H (6 mg/kg). BL, baseline. (**C**) Triazole 1.1 (24 mg/kg, ip) had no effect on frequency-rate curves (EF_{50}: $F_{4,53} = 0.3$, $P = 0.9$; R_{max}: $F_{4,53} = 0.6$, $P = 0.7$). (**D**) Dose-response comparisons are shown for EF_{50} (top) and R_{max} (bottom) compared to vehicle treatment (means ± SEM). No values were significantly different from vehicle, $\alpha = 0.05$. $n = 8$ to 13 rats for all groups and each graph in (A) to (D). BL data were obtained from all sessions before pharmacological manipulations and averaged for each subject, with the data shown being the between-subject means ± SEM. (**E**) Compound amounts detected in rat brain 30 min after U50,488H (6 mg/kg, ip) or triazole 1.1 (12 mg/kg, ip) shown as the means ± SEM of three rats per treatment.

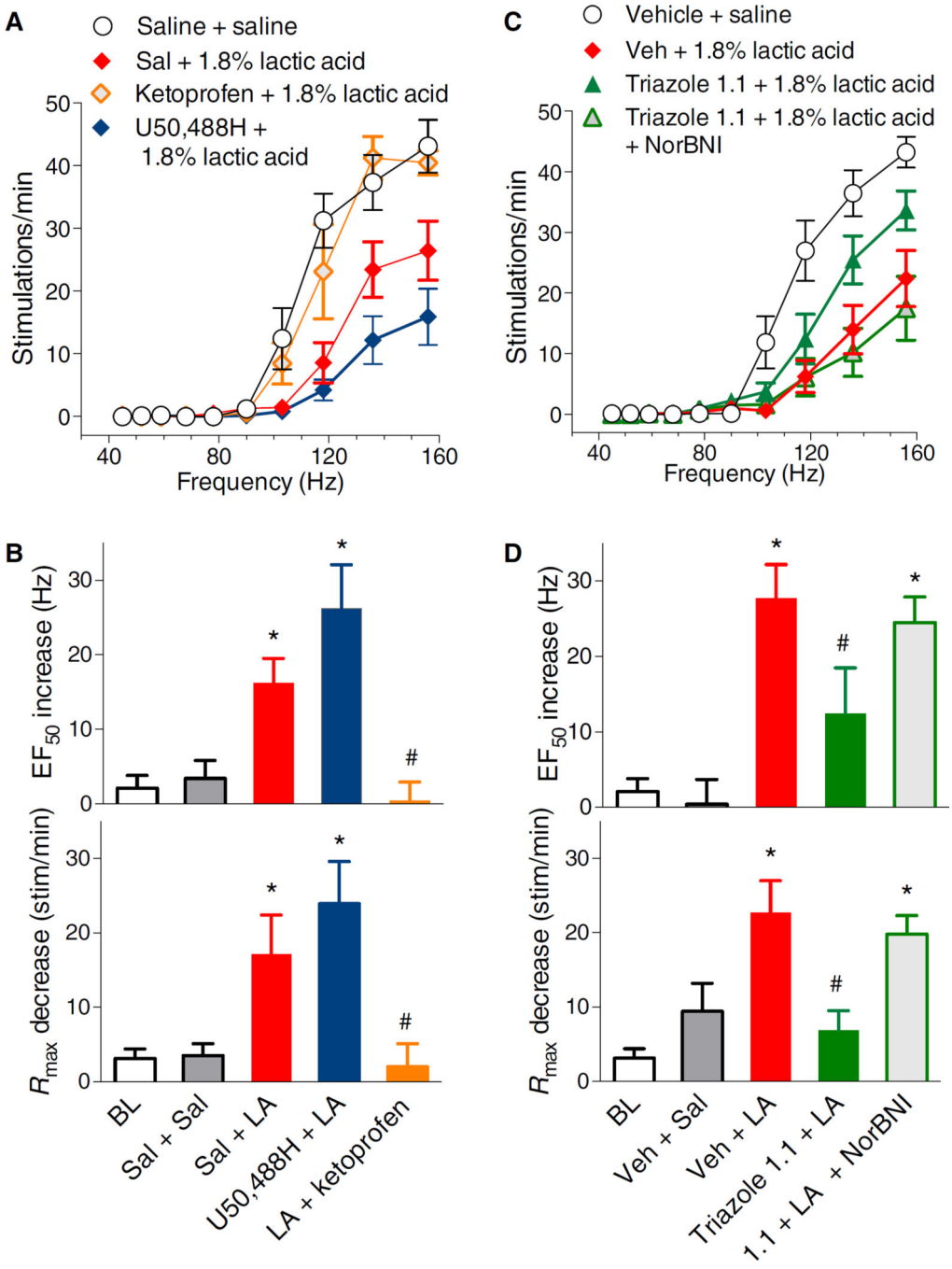

Fig. 6. Effects of ketoprofen, U50,488H, and triazole 1.1 on suppression of VTA ICSS by acute abdominal pain

(**A**) Intraperitoneal injection of 1.8% lactic acid (LA) decreased the maximal stimulations per minute ($F_{2,36}$ = 5.9, P = 0.006) and produced a rightward shift in frequency-rate curves (EF_{50}) ($F_{2,36}$ = 9.3, P = 0.0006) that was reversed by ketoprofen (1 mg/kg, sc) (EF_{50}: $F_{2,30}$ = 8.5, P = 0.001; R_{max}: $F_{2,30}$ = 4.6, P = 0.02 compared to lactic acid) but not by U50,488H (6 mg/kg, sc) (EF_{50}: $F_{2,34}$ = 8.2, P = 0.001; R_{max}: $F_{2,34}$ = 5.4, P = 0.009 compared to saline). (**B**) The effects on EF_{50} (top) and R_{max} (bottom) are summarized. One-way ANOVA for

drug effect indicates significance: $^{*}P \leq 0.05$ compared to saline + saline; $^{\#}P \leq 0.05$ compared to saline + 1.8% lactic acid. (**C**) Triazole 1.1 (24 mg/kg, ip) attenuated the response to 1.8% lactic acid injection (EF_{50}: $F_{2,26} = 9.7$, $P = 0.0007$; R_{max}: $F_{2,26} = 4.3$, $P = 0.02$) in a NorBNI (32 mg/kg, ip, 24 hours prior) reversible manner. (**D**) The effects on EF_{50} (top) and R_{max} (bottom) are summarized. One-way ANOVA for drug effect indicates significance: $^{*}P \leq 0.05$ significantly different from vehicle + saline, $^{\#}P \leq 0.05$ significantly different from vehicle + 1.8% lactic acid. $n = 8$ to 13 rats for all groups and all graphs in (A) to (D). Baseline (BL) data were obtained from all sessions before pharmacological manipulations and averaged for each subject, with the data shown being the between-subject means ± SEM.

Table 1

Pharmacological properties of Triazole 1.1, U50,488H, and U69,593.

Compound	[^{35}S]GTPγS binding assay				ΔΔLog*R*[*]
	EC_{50} (nM)	E_{max} (%)	Log*R*	ΔLog*R*	
U50,488H	24.0 ± 3	100	7.54 ± 0.06		0
U69,593	77.3 ± 9	114 ± 3	7.22 ± 0.07	−0.32 ± 0.04	−0.19 (−0.10 to −0.28)
Triazole 1.1	77.2 ± 18	101 ± 5	7.16 ± 0.11	−0.42 ± 0.03	1.44 (1.29 to 1.60)
	βarrestin2 enzyme fragment complementation assay				Bias factor *G*/β
	EC_{50} (nM)	E_{max} (%)	Log*R*	ΔLog*R*	($10^{\Delta\Delta Log R}$)
U50,488H	52.7 ± 3	100	7.27 ± 0.03	0	**1**
U69,593	64.7 ± 2	92 ± 2	7.14 ± 0.03	−0.13 ± 0.02	**0.6**
Triazole 1.1	4955 ± 542	98 ± 4	5.43 ± 0.04	−1.87 ± 0.05	**28**

[*](ΔLog*R* of [^{35}S]GTPγS − ΔLog*R* of βarrestin2 EFC) with 95% CI. The E_{max} of Triazole 1.1 was calculated at the highest tested concentration (30 μM) because of poor convergence for determining the median effective concentration (EC_{50}) in the βarrestin2 assay. $n \geq 4$ experiments performed in duplicate, with the reference compound (U50,488H) run in parallel with each test ligand within each experiment.